

## ARTICLE

# A Minimal Physiologically-Based Pharmacokinetic Model for Tacrolimus in Living-Donor Liver Transplantation: Perspectives Related to Liver Regeneration and the *cytochrome P450 3A5 (CYP3A5)* Genotype

Kotaro Itohara<sup>1,2</sup>, Ikuko Yano<sup>1,3,\*</sup>, Tetsunori Tsuzuki<sup>1</sup>, Miwa Uesugi<sup>1</sup>, Shunsaku Nakagawa<sup>1</sup>, Atsushi Yonezawa<sup>1,2</sup> , Hideaki Okajima<sup>4</sup>, Toshimi Kaido<sup>4</sup>, Shinji Uemoto<sup>4</sup> and Kazuo Matsubara<sup>1</sup>

In adult patients after living-donor liver transplantation, postoperative days and the *cytochrome P450 3A5 (CYP3A5)* genotype are known to affect tacrolimus pharmacokinetics. In this study, we constructed a physiologically-based pharmacokinetic model adapted to the clinical data and evaluated the contribution of liver regeneration as well as hepatic and intestine *CYP3A5* genotypes on tacrolimus pharmacokinetics. As a result, liver function recovered immediately and affected the total body clearance of tacrolimus only during a limited period after living-donor liver transplantation. The clearance was about 1.35-fold higher in the recipients who had a liver with the *CYP3A5\*1* allele than in those with the *CYP3A5\*3/\*3* genotype, whereas bioavailability was ~0.7-fold higher in the recipients who had intestines with the *CYP3A5\*1* allele than those with *CYP3A5\*3/\*3*. In conclusion, the constructed physiologically-based pharmacokinetic model clarified that the oral clearance of tacrolimus was affected by the *CYP3A5* genotypes in both the liver and intestine to the same extent.

## Study Highlights

**WHAT IS THE CURRENT KNOWLEDGE ON THE TOPIC?**

☑ In living-donor liver transplantation, the respective *cytochrome P450 3A5 (CYP3A5)* genotypes in the liver and small intestine from the donor and recipient, respectively, and the number of postoperative days can affect tacrolimus metabolism.

**WHAT QUESTION DID THIS STUDY ADDRESS?**

☑ This study evaluated the quantitative contributions of hepatic and intestinal *CYP3A5* genotypes and liver regeneration in living-donor liver transplant patients using physiologically-based pharmacokinetic modeling and clinical data application.

**WHAT DOES THIS STUDY ADD TO OUR KNOWLEDGE?**

☑ The constructed physiologically-based pharmacokinetic model describes rapid recovery of liver function after living-donor liver transplantation and the same effect of the *CYP3A5* genotypes both in the liver and intestine on the oral clearance of tacrolimus.

**HOW MIGHT THIS CHANGE DRUG DISCOVERY, DEVELOPMENT, AND/OR THERAPEUTICS?**

☑ The oral clearance could be classified into three patterns according to the *CYP3A5* genotype combination of the donor and recipient. The recommended initial dosage of tacrolimus guided by genotype using physiologically-based pharmacokinetic simulations would be useful to maintain the therapeutic range quickly.

Tacrolimus is used as a key immunosuppressant in several organ transplantations, and the therapeutic drug monitoring (TDM) of this compound is important to prevent rejections or adverse effects because tacrolimus has a narrow therapeutic range and large interindividual and intraindividual variabilities.<sup>1–4</sup> Tacrolimus is rapidly absorbed after oral administration, but its oral bioavailability (*F*) is

poor.<sup>2</sup> Tacrolimus is metabolized by cytochrome P450 3A4 (*CYP3A4*) as well as cytochrome P450 3A5 (*CYP3A5*) in the liver and small intestine.<sup>2</sup> Genetic polymorphisms of *CYP3A5* include the wild-type allele *CYP3A5\*1* and the variant allele *CYP3A5\*3*.<sup>5</sup> The wild-type allele *CYP3A5\*1* produces high levels of full-length *CYP3A5* messenger RNA and expresses high levels of the functional *CYP3A5* protein

<sup>1</sup>Department of Clinical Pharmacology and Therapeutics, Kyoto University Hospital, Kyoto Japan; <sup>2</sup>Graduate School of Pharmaceutical Sciences, Kyoto University, Kyoto, Japan; <sup>3</sup>Department of Pharmacy, Kobe University Hospital, Kobe, Japan; <sup>4</sup>Division of Hepato-Biliary-Pancreatic Surgery and Transplantation, Department of Surgery, Graduate School of Medicine, Kyoto University, Kyoto, Japan. \*Correspondence: Ikuko Yano (iyano@med.kobe-u.ac.jp)

Received: March 22, 2019; accepted: April 19, 2019. doi:10.1002/psp4.12420

(CYP3A5 expressor), whereas the variant *CYP3A5\*3/\*3* produces very low or undetectable levels of the functional CYP3A5 protein (CYP3A5 nonexpressor).<sup>5</sup> Tacrolimus is a substrate of P-glycoprotein multidrug resistance protein 1 (MDR1)/ATP-binding cassette sub-family B member 1 (ABCB1), which actively transports tacrolimus back into the intestinal lumen and affects the *F* of this drug.<sup>6</sup> The total body clearance (CL), volume of distribution, and *F* of blood tacrolimus in healthy volunteers were reported as 0.040 L/hour/kg, 1.91 L/kg, and 17.8%, respectively.<sup>7</sup>

Liver transplantation is a treatment for patients with end-stage liver disease. Because of the organ shortage for transplantation, the typical liver transplantation in Japan is living-donor liver transplantation (LDLT). In LDLT, about 30–60% of the liver from the donor is harvested and transplanted to the recipient.<sup>8</sup> The liver has a strong ability to regenerate, and it can become a nearly suitable size within a few months after transplantation.<sup>9–12</sup> Previous reports have shown that patients who performed LDLT show smaller CL values than patients who received kidney or cadaveric liver transplantation, and the CL value increased with postoperative days (POD) to establish a steady state within 30 days of surgery.<sup>13–15</sup> Interestingly, in patients with a liver transplantation, the *CYP3A5* genotypes in the liver and small intestine are derived from the donor and recipient, respectively. Therefore, POD and *CYP3A5* genotypes in the grafted liver and small intestine of recipients can mutually affect the pharmacokinetics of tacrolimus in LDLT patients. Previous reports showed that the trough blood concentration/dose (C/D) ratio of tacrolimus was significantly lower in the recipients who had a liver or an intestine with the *CYP3A5\*1* allele than those with the *CYP3A5\*3/\*3* genotype.<sup>16</sup> We previously reported that the intestinal *CYP3A5\*1* allele, but not the liver *CYP3A5\*1* allele, affected the individual oral CL (CL/*F*) of tacrolimus in adult LDLT recipients by the population pharmacokinetic analysis.<sup>17</sup>

Physiologically-based pharmacokinetic (PBPK) models have been used as a tool to quantitatively evaluate the effect of the physiological change on drug disposition.<sup>18</sup>

The following two approaches are usually used for model building:<sup>19</sup> (i) the “top-down” approach that uses observed clinical data to build the model, and (ii) the “bottom-up” approach that uses drug-specific and system-specific data to build the model. Although these two approaches have been employed for research studies, a better model may be established by combining these two known models, namely, a middle-out approach.<sup>20</sup>

In this study, we quantitatively evaluated the effects of liver regeneration as well as hepatic and intestinal *CYP3A5* genotypes on tacrolimus pharmacokinetics in LDLT patients using a PBPK model based on clinical data to estimate the appropriate initial tacrolimus dosage in LDLT patients.

## METHODS

### Clinical data

A total of 26 adult LDLT patients receiving initial intravenous injection of tacrolimus followed by the oral administration at Kyoto University Hospital (from December 2013–January 2016) were included in the model-building data used to develop the present PBPK model for tacrolimus. The blood sampling was performed in the morning and/or in the evening daily during the intravenous infusion period and at the trough point during the oral administration period as part of routine TDM. In addition, a total of 272 adult patients receiving tacrolimus therapy during 4 weeks after LDLT at Kyoto University Hospital (from July 2004–June 2011) were included in the verification data for evaluating the constructed PBPK model. The blood sampling times of the verification data were all trough points. The patients’ ages in the verification data were 20 years old and older and were included in a previous report by Uesugi *et al.*<sup>16</sup> **Table S1** shows the characteristics of the LDLT patients in this study.

The blood concentration of tacrolimus was measured using a microparticle enzyme-linked immunoassay (IMx; Abbott, Tokyo, Japan) between July 2004 and March 2009 and a chemiluminescent enzyme immunoassay (ARCHITECT; Abbott) after April 2009. The equivalence of the data obtained using these two methods was validated in our hospital.<sup>21</sup>

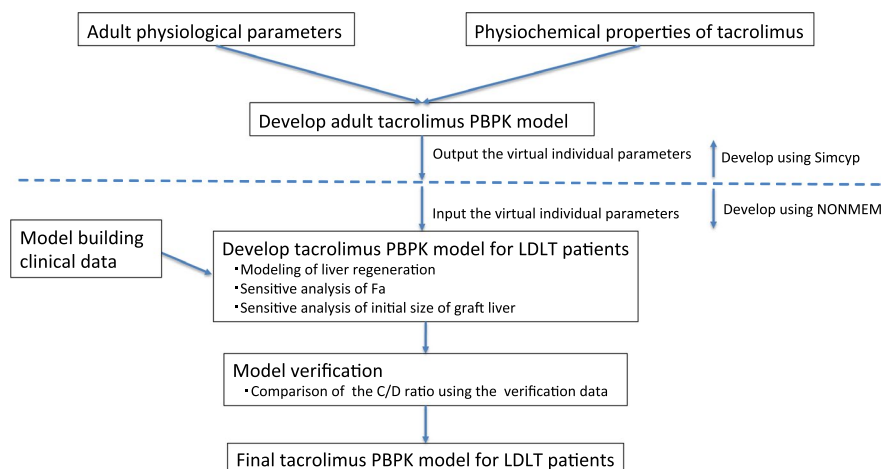


**Figure 1** Physiologically-based pharmacokinetic (PBPK) modeling workflow used in this study. C/D, concentration/dose; Fa, fraction of dose absorbed; LDLT, living-donor liver transplantation.

This study was carried out in accordance with the Declaration of Helsinki and its amendments and was approved by the Ethics Committee of Kyoto University Graduate School, Faculty of Medicine and Kyoto University Hospital (Kyoto, Japan).

### PBPK model development of tacrolimus for LDLT patients

The workflow for tacrolimus PBPK modeling is shown in **Figure 1**. Simcyp population-based absorption, distribution, metabolism, and excretion simulator version 17 (Certara, Sheffield, UK) was used to build the PBPK model of tacrolimus. The drug parameter values of tacrolimus and the population mean physiological parameter values used to build the PBPK model<sup>22–26</sup> are shown in **Table S2**. Pharmacokinetic parameters for tacrolimus were described based on the blood concentrations. Physiological parameters such as body weight and cardiac output were based on the default Japanese population data provided by the simulator, whereas the mean hematocrit value was changed from the default value in the Simcyp to 25.5% based on our clinical data. In addition, according to the literature, the mean abundances of CYP3A4 and CYP3A5 in the liver were changed from the default values in the Simcyp to 93 and 17 pmol/mg, respectively, and these coefficient of variation (CV) values were in turn changed to 81 and 185%, respectively.<sup>26</sup> Because the clinical data using the model building were not rich sampling data and our objective was to know the initial dose of tacrolimus in LDLT patients based on the genotype information, the minimal PBPK model was selected in this study. The volume of distribution in blood was set as 1.29 L/kg according to the preanalysis of model-building data. The fraction of drug unbound in the gut was fixed to 1, according to the result of sensitive analysis about the fraction of drug unbound in the gut vs. *F* (**Figure S1**).

### Construction of liver regeneration model

Because the liver regeneration profile could not directly be modeled in the Simcyp simulator, the output data of simulated virtual individual parameters by Simcyp were used as the input data into the nonlinear mixed effects modeling (NONMEM) program version 7.2 (ICON, Ellicott City, MD; **Figure 1**). In addition, the equations used in Simcyp (shown in **Supplementary Information**) were also incorporated based on a one-compartment with first-order absorption model with conditional estimation to reproduce the time-concentration data, and the code is shown in **Supplementary Information**. We confirmed that NONMEM reproduced the predicted blood concentrations of tacrolimus corresponding to the predicted blood concentration of tacrolimus using Simcyp, and the subsequent simulation was performed using NONMEM.

Several liver regeneration models were incorporated into the model equation in NONMEM. The previous literature reported results concerning liver regeneration after LDLT. In one study, the grafted liver doubled within 1 week,<sup>11</sup> whereas in another, the liver regenerated to the recipient standard liver size in 1 month.<sup>12</sup> Because of the discrepancies in the measurement frequency of the liver size among

the published reports, we could not determine the precise liver regeneration profile. Therefore, in this study, we first compared the various liver regeneration models (such as Eqs. 1–4) to explore the model best fits in the clinical data. In Eqs. 1–4, LWstd and GR represent the recipient standard liver weight in each patient generated by Simcyp and the ratio of grafted to the recipient standard liver weight, respectively. At first, GR was assumed to be 60% in all of the models.

$$LW = \left( GR + \frac{1-GR}{1+(1/POD)} \right) * LWstd (g) \quad (1)$$

$$\begin{cases} LW = \left( GR + \frac{1-GR}{7} * POD \right) * LWstd (0 \leq POD \leq 7) \\ LW = LWstd (POD > 7) \end{cases} \quad (g) \quad (2)$$

$$\begin{cases} LW = \left( GR + \frac{1-GR}{14} * POD \right) * LWstd (0 \leq POD \leq 14) \\ LW = LWstd (POD > 14) \end{cases} \quad (g) \quad (3)$$

$$\begin{cases} LW = \left( GR + \frac{1-GR}{30} * POD \right) * LWstd (0 \leq POD \leq 30) \\ LW = LWstd (POD > 30) \end{cases} \quad (g) \quad (4)$$

The raw blood concentration in the model-building data is shown in **Figure S2**. Because the observed blood concentration varied widely and both the period and dose of intravenous administration of tacrolimus were different in each patient, the simulated blood concentrations of tacrolimus immediately after LDLT (considering the liver regeneration using Eqs. 1–4) were compared with the observed concentrations normalized by the dosing regimen to identify the best-fit liver-regeneration model. The dosing regimen used for the normalization was set to the initial protocol at Kyoto University Hospital in 2013. Briefly, tacrolimus was intravenously administered at a rate of 1.25 µg/hour/kg during the first 12 hours and then was reduced to 0.83 µg/hour/kg before switching to oral administration of 0.04 mg/day/kg 3 days after transplantation. Each observed concentration was normalized to this dosing regimen by using the *post hoc* Bayesian method using NONMEM; namely, the individual pharmacokinetic parameters were estimated by using the Bayesian method, where the population pharmacokinetic parameters were obtained from the one-compartment model constructed based on in-house data including model-building data and pediatric patient data in the same observed period (T. Tsuzuki, A. Yonezawa, and K. Matsubara, unpublished data). The mean value and interindividual variability (CV) for the population pharmacokinetic parameters of CL and volume of distribution were 1.16 L/hour and 36% and 1.29 L/kg and 41%, respectively. CYP3A5 genotype combinations of the liver and small intestine were as follows: CYP3A5\*1 allele in both the graft liver and small intestine (L\*1/I\*1), CYP3A5\*1 allele in the graft liver and CYP3A5\*3/\*3 in the small intestine (L\*1/I\*3), CYP3A5\*3/\*3 in the graft liver and CYP3A5\*1 allele in the small intestine (L\*3/I\*1), and CYP3A5\*3/\*3 in both the graft liver and small intestine (L\*3/I\*3).

Using the individual parameters of the Japanese vertical population generated by Simcyp to NONMEM, the

time-concentration profiles of 100 virtual adult Japanese were calculated for each *CYP3A5* genotype combination of liver and small intestine. The squared error (SQE) and the root mean square error (RMSE) as described in Eqs. 5 and 6 were calculated as the model precision index as follows:<sup>27</sup>

$$\text{SQE} = (\text{MED} - \text{IOBS}_i)^2 \quad (5)$$

$$\text{RMSE} = \sqrt{\frac{1}{N} \sum_{i=1}^N (\text{SQE})} \quad (6)$$

where MED is the median value of blood concentration simulated by the PBPK model,  $\text{IOBS}_i$  represents the observed concentrations normalized to the dosing regimen, and  $N$  denotes the number of blood samples.

After construction of the liver-generation model, we examined the effects of fraction of dose absorbed ( $F_a$ ) values of 0.8, 0.6, and 0.4 to explore a better-fitting model.

Statistical analysis was performed between the SQE of each model using one-way analysis of variance.  $P$  value < 0.05 was considered to be significant. In addition, the absolute value of RMSE was compared among models, and the model showing the smallest RMSE value was selected as the best-fitting model.

Finally, the effect of the initial value of the graft liver size was examined using the selected best-fitting model.

### Simulation

As in the model-building step, the tacrolimus concentration data in 100 virtual adult Japanese were calculated for each *CYP3A5* genotype combination to evaluate the effect of liver regeneration and the *CYP3A5* genotype. At first, blood concentrations of tacrolimus immediately after LDLT and the C/D

ratio during 1 month after LDLT for each *CYP3A5* genotype combination were simulated. In this simulation, tacrolimus was intravenously administered at a rate of 1.25  $\mu\text{g}/\text{hour}/\text{kg}$  during the first 12 hours and then reduced to 0.83  $\mu\text{g}/\text{hour}/\text{kg}$ . At 3 days after transplantation, tacrolimus was switched to oral administration at a dose of 0.04 mg/day/kg. Simulated blood concentrations after LDLT were first compared with the model-building clinical data. Then, C/D ratios after LDLT were compared with the verification clinical data for model evaluation. Finally, using the final model, CL,  $F$ , and CL/ $F$  of tacrolimus during post-LDLT 1 month for each *CYP3A5* genotype combination were calculated.

Finally, the recommended dose for each *CYP3A5* genotype was calculated by using the final model. Briefly, the loading dose that brings the blood concentration of tacrolimus to 15 ng/mL after 12 hours after intravenous infusion, the maintenance dose 12 hours after the infusion that maintains the blood concentration of 15 ng/mL, and the oral administration dosage that maintains the trough concentration at 10 ng/mL were calculated, respectively.

## RESULTS

### PBPK modeling

Regarding the effect of liver regeneration on the blood concentration of tacrolimus (Figure 2), the median SQE values using each model (Eqs. 1–4) were 12.8 (90% confidence interval (CI): 0.164–185), 15.4 (90% CI: 0.136–240), 37.7 (90% CI: 0.741–343), and 66.1 (90% CI: 0.853–393), respectively, and the SQE value using Eq. 1 was significantly different when compared with the other models (Eqs. 2–4;  $P < 0.001$ ). However, the predicted values were slightly higher when compared with the observed concentrations normalized to the dosing regimen in all *CYP3A5* genotype combinations using Eq. 1.

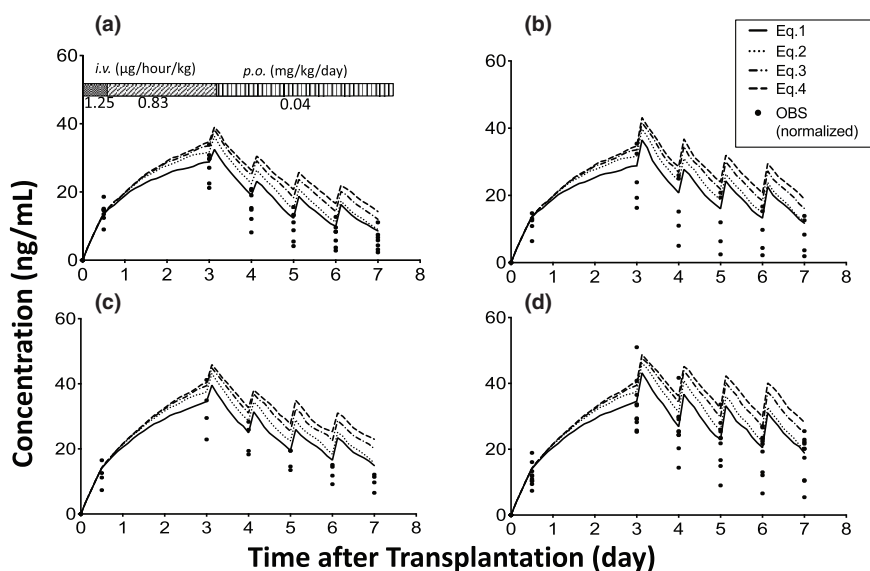


**Figure 2** Effect of liver regeneration rate on the blood concentration of tacrolimus immediately after living-donor liver transplantation. (a) cytochrome P450 3A5 (*CYP3A5*)\*1 allele in both the graft liver and small intestine ( $L^*1/I^*1$ ), (b) *CYP3A5*\*1 allele in the graft liver and *CYP3A5*\*3/\*3 in the small intestine ( $L^*1/I^*3$ ), (c) *CYP3A5*\*3/\*3 in the graft liver and *CYP3A5*\*1 allele in the small intestine ( $L^*3/I^*1$ ), and (d) *CYP3A5*\*3/\*3 in both the graft liver and small intestine ( $L^*3/I^*3$ ). Each closed circle shows the observed concentration normalized by the dosing regimen (OBS). The number of patients with  $L^*1/I^*1$ ,  $L^*1/I^*3$ ,  $L^*3/I^*1$ , and  $L^*3/I^*3$  were 7, 5, 4, and 10, respectively. i.v., intravenous; p.o., per oral.

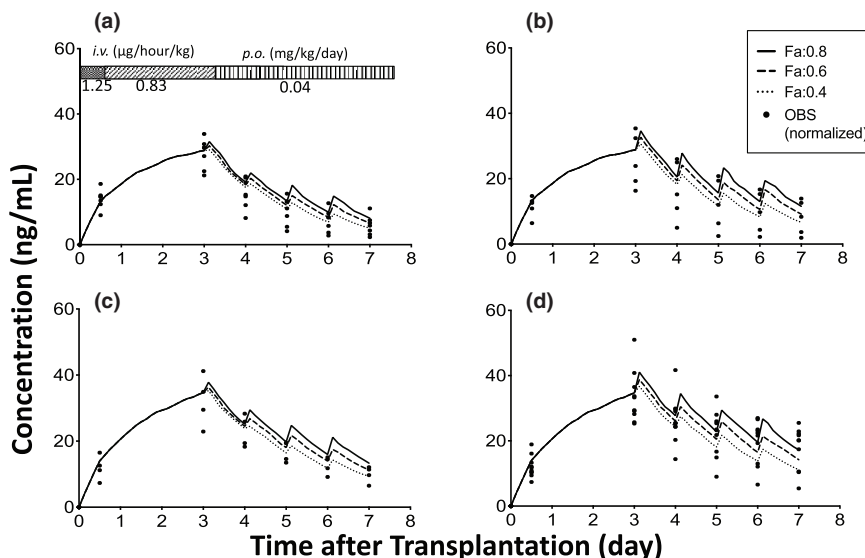


**Figure 3** Effect of a fraction of dose absorbed ( $F_a$ ) on the blood concentration of tacrolimus immediately after living-donor liver transplantation. (a) *cytochrome P450 3A5 (CYP3A5)\*1* allele in both the graft liver and small intestine ( $L^*1/I^*1$ ), (b)  $CYP3A5^*1$  allele in the graft liver and  $CYP3A5^*3/*3$  in the small intestine ( $L^*1/I^*3$ ), (c)  $CYP3A5^*3/*3$  in the graft liver and  $CYP3A5^*1$  allele in the small intestine ( $L^*3/I^*1$ ), and (d)  $CYP3A5^*3/*3$  in both the graft liver and small intestine ( $L^*3/I^*3$ ). Each closed circle shows the observed concentration normalized by the dosing regimen (OBS). The number of patients with  $L^*1/I^*1$ ,  $L^*1/I^*3$ ,  $L^*3/I^*1$ , and  $L^*3/I^*3$  were 7, 5, 4, and 10, respectively. i.v., intravenous; p.o., per oral.

Next, we examined the effect of  $F_a$  on the predicted blood concentration of tacrolimus (**Figure 3**), and the results showed that the median SQE values using the  $F_a$  values of 0.8, 0.6, and 0.4 were 13.9 (90% CI: 0.0524–174), 14.7 (90% CI: 0.221–142), and 16.5 (90% CI: 0.0607–177), respectively. There were no statistically significant differences between each group. The RMSE values using the  $F_a$  values of 0.8, 0.6, and 0.4 were 5.84 (90% CI: 5.16–6.46), 5.69 (90% CI: 5.08–6.35), and 6.03 (90% CI: 5.34–6.73), respectively. We subsequently selected the  $F_a$  value of 0.6 because it yielded the smallest RMSE value.

Using the selected model (Eq. 1 and  $F_a$  value of 0.6), the graft liver size had little effect on the predicted concentrations (**Figure S3**).

#### Model verification

Approximately 95% of the observed blood concentrations normalized by the standard dosage regimens immediately after LDLT were within one standard deviation of that predicted by the final model (**Figure 4**).

Furthermore, most of the observed C/D ratios during the 28 days after LDLT in the verification data were within the 90% CI of the predicted values for each  $CYP3A5$  genotype combination in each period (**Figure 5**). For example, the median values of the C/D ratio predicted by the constructed PBPK model were 102, 155, 167, and 244 (ng/mL)/(mg/kg), and the CV values were 75, 77, 101, and 94% for POD 22–28 in patients who had  $L^*1/I^*1$ ,  $L^*1/I^*3$ ,  $L^*3/I^*1$ , and  $L^*3/I^*3$ , respectively. The median values of the observed C/D ratio were 123, 173, 121, and 193 ng/mL/mg/kg, and the CV values were 66, 139, 127, and 113% for POD 22–28 in patients who had  $L^*1/I^*1$ ,  $L^*1/I^*3$ ,  $L^*3/I^*1$ , and  $L^*3/I^*3$ , respectively.

#### Simulation

The simulation using the final PBPK model showed that the CL increased immediately after LDLT and subsequently reached 1.59 and 1.19 L/hour in patients who had a graft liver with the  $CYP3A5^*1$  allele ( $L^*1$ ) and  $CYP3A5^*3/*3$  ( $L^*3$ ), respectively (**Figure 6**). The  $F$  values in patients who had a small intestine with the  $CYP3A5^*1$  allele ( $I^*1$ ) and  $CYP3A5^*3/*3$  ( $I^*3$ ) registered 0.090 and 0.131, respectively. The breakdown of  $F$  was as expressed as follows:  $F_a$  was designated the same value (0.6) for all  $CYP3A5$  genotype combinations. Hepatic availability ( $F_h$ ) values in patients who had  $L^*1$  and  $L^*3$  indicated 0.979 and 0.985, respectively. Intestinal availability ( $F_g$ ) values in patients who had  $I^*1$  and  $I^*3$  showed 0.153 and 0.227, respectively. The CL/ $F$  values increased immediately after LDLT and subsequently reached 17.0, 11.3, 11.8, and 7.9 L/hour in patients with  $L^*1/I^*1$ ,  $L^*1/I^*3$ ,  $L^*3/I^*1$ , and  $L^*3/I^*3$ , respectively. The recommended dosage was calculated based on the final PBPK model (**Table 1**).

#### DISCUSSION

The present minimal PBPK model using clinical data quantitatively evaluated the contribution of hepatic and intestinal  $CYP3A5$  genotypes to the CL,  $F$ , and CL/ $F$  values. The PBPK model showed that the CL was affected by the  $CYP3A5$  genotype in the liver and the  $F$  was affected by the  $CYP3A5$  genotype in the small intestine. Therefore, the initial dosage of tacrolimus can be selected based on  $CYP3A5$  genotypes in the recipient and donor in LDLT. The recommended dosage of tacrolimus guided by genotype using PBPK simulations would be useful to quickly maintain blood concentrations within the therapeutic range.

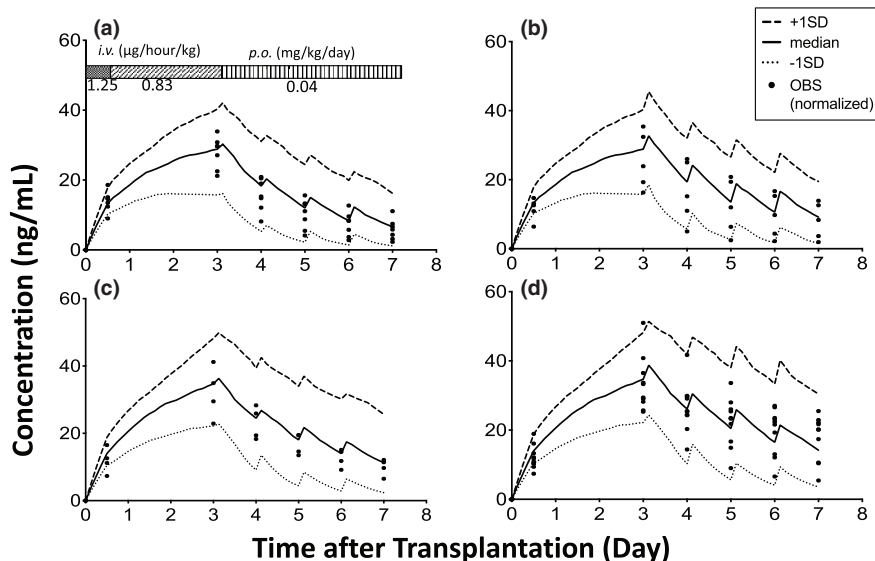


**Figure 4** Effect of cytochrome P450 3A5 (CYP3A5) genotypes on the blood concentration of tacrolimus immediately after living-donor liver transplantation. (a) CYP3A5\*1 allele in both the graft liver and small intestine (L\*1/I\*1), (b) CYP3A5\*1 allele in the graft liver and CYP3A5\*3/\*3 in the small intestine (L\*1/I\*3), (c) CYP3A5\*3/\*3 in the graft liver and CYP3A5\*1 allele in the small intestine (L\*3/I\*1), and (d) CYP3A5\*3/\*3 in both the graft liver and small intestine (L\*3/I\*3). Each closed circle shows the observed concentration normalized by the dosing regimen (OBS). The number of patients with L\*1/I\*1, L\*1/I\*3, L\*3/I\*1, and L\*3/I\*3 were 7, 5, 4, and 10, respectively. SD, standard deviation. i.v., intravenous; p.o., per oral.

In the Simcyp simulator, the default value of the mean abundance of CYP3A4 in the liver in the Japanese population was designated as 122 pmol/mg. In addition, the default value of the mean abundance of CYP3A5 in the liver was proportional to the abundance of CYP3A4 in the liver.<sup>25,28–30</sup> Using these default values, the median CL/F in patients with L\*1/I\*1 and L\*3/I\*3 were 57.4 and 13.2 L/hour, respectively. Therefore, the CL/F in patients with L\*1/I\*1 was about quadrupled when compared with the CL/F in patients with L\*3/I\*3. However, some studies on the population pharmacokinetics of tacrolimus in renal transplantation have been published in which the CL/F values in patients with the CYP3A5\*1 allele and CYP3A5\*3/\*3 are 20.9–54.5 and 15.4–27.3 L/hour, respectively, and the CL/F value in patients who have the CYP3A5\*1 allele registers 1.12–2.07 times higher than those with the CYP3A5\*3/\*3 allele.<sup>31–40</sup> It was possible that CL/F would be calculated considerably higher when using the default values of the mean abundance from CYP3A4 and CYP3A5. Therefore, we decided to use the values described in the literature of the abundance of CYP3A4 and CYP3A5 in the liver based on the results of a meta-analysis.<sup>26</sup>

In this PBPK simulation, the CL of tacrolimus ~35% higher in recipients who had L\*1 than those with L\*3. In addition, *F* was about 30% lower in the recipients who had I\*1 than those with I\*3, whereas hardly any difference in *F* was observed between the patients who had L\*1 and those with L\*3 (Figure 6). Therefore, because the first-pass metabolism of tacrolimus mainly occurred in the small intestine (not in the liver), the small-for-size graft and liver regeneration did not affect the *F* value of tacrolimus in the LDLT patients. Consequently, the CL/F of tacrolimus was affected by the CYP3A5 genotypes in both the liver and intestine to approximately the same degree.

The PBPK-simulated mean CL in patients who had L\*1 and L\*3 were 0.975 and 0.729 on POD 0 and increased to 1.59 and 1.19 L/hour on day 30, respectively (Figure 6a). Fukatsu et al.<sup>15</sup> reported that the respective population mean estimates for CL on PODs 0 and 30 are 0.737 and 1.14 L/hour, and the CL of tacrolimus was increased linearly according to POD. The PBPK-simulated CL value derived in our study was considered reasonable, but the best-fit model was obtained in Eq. 1. Therefore, the liver function would be recovered immediately in the early period after LDLT.

In our study, the PBPK-simulated mean *F* value in patients with I\*1 and I\*3 are 0.090 and 0.131, respectively. As the reported values of *F* vary from 0.0677–0.28,<sup>15,41–43</sup> the PBPK-simulated *F* values derived in our study were considered reasonable. When the *F*<sub>a</sub> value was changed to 0.6, the model had the best fit to the observed concentrations. However, *F*<sub>a</sub> and *F*<sub>g</sub> could not be separated accurately in this study. In healthy volunteers, the *F*<sub>h</sub> and *F*<sub>a</sub>\**F*<sub>g</sub> values of tacrolimus were reported as 96% and 14%, respectively.<sup>44</sup> The PBPK-simulated mean *F*<sub>h</sub> value in patients with L\*1 and L\*3 were 0.967 and 0.976, respectively, consistent with the literature value.<sup>31,44</sup> Therefore, the 40% reduction of *F*<sub>a</sub> might be a result of the *F*<sub>a</sub>\**F*<sub>g</sub> reduction by increasing the gut metabolism by the function of P-glycoprotein because we did not include the P-glycoprotein efflux mechanism in the present PBPK model. In addition, we considered that the different circumstance in liver transplantation might affect the absorption of tacrolimus. Because tacrolimus is classified as biopharmaceutics classification system class II,<sup>45</sup> where drugs have low solubility and high membrane permeability, its absorption is possibly affected by bile. Because bile is excreted outside the body by drainage in patients after LDLT, we considered that the *F*<sub>a</sub> of tacrolimus in LDLT

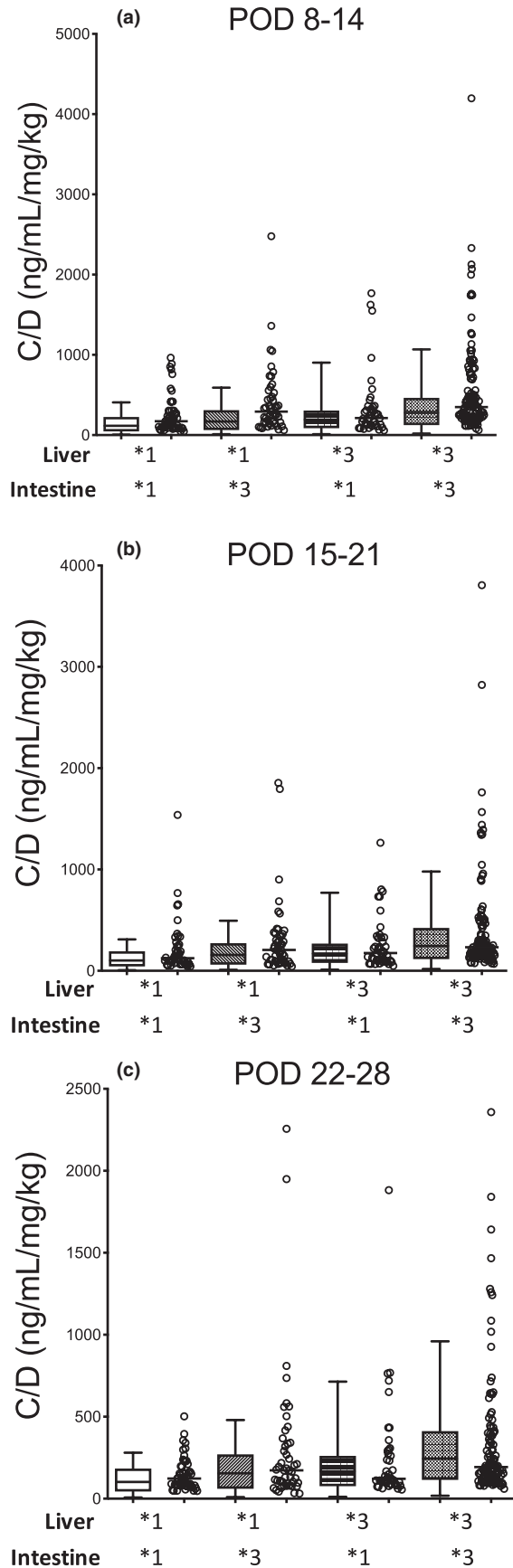


**Figure 5** Comparison of the physiologically-based pharmacokinetic-simulated and observed concentration of verification data divided by the concentration/dose (C/D) ratios of tacrolimus in each *cytochrome P450 3A5 (CYP3A5)* genotype combination of graft liver and small intestine for PODs (a) 8–14, (b) 15–21, and (c) 22–28 after living-donor liver transplantation. Each box plot represents the interquartile range and 90% confidence interval of the predicted C/D ratio. Each open circle shows the observed C/D ratio, and each bar shows the median value. The number of patients with *CYP3A5\*1* allele in both the graft liver and small intestine, *CYP3A5\*1* allele in the graft liver and *CYP3A5\*3/3* in the small intestine, *CYP3A5\*3/3* in the graft liver and *CYP3A5\*1* allele in the small intestine, and *CYP3A5\*3/3* in both the graft liver and small intestine were 54, 52, 47, and 119, respectively. POD, postoperative day.

patients might be decreased because of the absence of bile and/or the insufficient bowel moving after the operation. On one hand, the CL/F values in renal transplant patients with the *CYP3A5\*1* allele and *CYP3A5\*3/3* were 20.9–54.5 and 15.4–27.3 L/hour, respectively.<sup>31–40</sup> These values were higher when compared with our results; therefore we considered that the liver function might not be completely recovered in LDLT patients within 30 days after the operation.

The C/D ratios using the verification clinical data had large interindividual variability, showing the CV values of 66, 139, 127, and 113% in patients who had *L\*1/I\*1*, *L\*1/I\*3*, *L\*3/I\*1*, and *L\*3/I\*3*, respectively in PODs 22–28 (Figure 5). On one hand, the CV values of PBPK-simulated C/D ratios were 75, 77, 101, and 94% in patients who had *L\*1/I\*1*, *L\*1/I\*3*, *L\*3/I\*1*, and *L\*3/I\*3* for PODs 22–28, respectively. These results showed that the CV values derived from the observed C/D ratios using the verification data were slightly greater than those of the PBPK-simulated C/D ratio. This tendency was also seen in PODs 8–14 and 15–21. Although hematocrit is reported as a covariate of tacrolimus CL,<sup>38</sup> the hematocrit value was fixed in our simulation studies. We considered this as one of factors yielding larger interindividual variability in the observed C/D ratios when compared with the PBPK simulations.

The loading dose in patients who had *L\*1* and those with *L\*3* were calculated as 1.41 and 1.31  $\mu\text{g}/\text{hour}/\text{kg}$ , respectively, which were not so different (Table 1). This is because the loading rate was much faster than the tacrolimus CL itself, and the blood concentration 12 hours after the transplantation depends on the volume of distribution, but not CL, of tacrolimus. On the other hand, the maintenance dose depends on the CL, and it is necessary to adjust based on the liver regeneration. The recommended oral dose as times increase when compared with the maintenance intravenous dose should be changed depending on the *CYP3A5* genotype in the small intestine. Although information on the genotype-guided initial dosing design is useful, the individual dosage should be changed based on the TDM measurements because of the large interindividual and intraindividual variabilities of tacrolimus pharmacokinetics.

There are some limitations acknowledged in this study. First, we constructed and evaluated the minimal PBPK model of tacrolimus using routine TDM data consisting of almost trough blood concentrations. Although we could not evaluate more complicated models in the absorption process and could not separate  $F_a$  and  $F_g$  accurately, it would

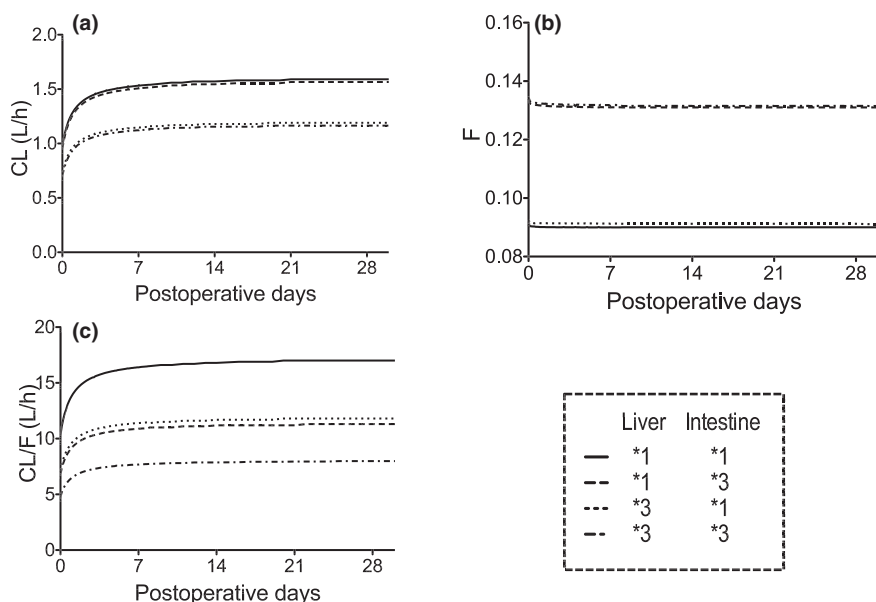


**Figure 6** Physiologically-based pharmacokinetic-simulated (a) median clearance (CL), (b) bioavailability (F), and (c) oral clearance (CL/F) of tacrolimus during 28 days after living-donor liver transplantation for each cytochrome P450 3A5 (CYP3A5) genotype combination of graft liver and small intestine.

**Table 1** Recommend dosage in each CYP3A5 genotype

Genotype combination	L*1/I*1	L*1/I*3	L*3/I*1	L*3/I*3
Intravenous infusion				
Loading dose, $\mu\text{g}/\text{hour}/\text{kg}$	1.41	1.41	1.31	1.31
Maintenance dose, $\mu\text{g}/\text{hour}/\text{kg}$ (at POD 0.5)	0.309	0.309	0.230	0.230
Oral administration dosing				
Oral dose, $\text{mg}/\text{day}/\text{kg}$ (or times increase compared with maintenance intravenous dose) (at POD 3)	0.0662 (8.93)	0.0446 (6.01)	0.0468 (8.47)	0.0306 (5.54)

The loading dose was calculated to bring the blood concentration to 15 ng/mL at 12 hours after intravenous infusion. The maintenance dose was calculated to maintain the blood concentration of 15 ng/mL 12 hours after the transplantation. The oral dose was calculated compared with the intravenous maintenance dose to maintain trough concentration at 10 ng/mL at POD 3. L\*1/I\*1, L\*1/I\*3, L\*3/I\*1, and L\*3/I\*3 represent CYP3A5\*1 allele in both the graft liver and small intestine, CYP3A5\*1 allele in the graft liver and CYP3A5\*3/\*3 in the small intestine, CYP3A5\*3/\*3 in the graft liver and CYP3A5\*1 allele in the small intestine, and CYP3A5\*3/\*3 in both the graft liver and small intestine, respectively. CYP3A5, cytochrome P450 3A5; POD, postoperative day.

be important to examine in detail the effects of gut metabolism or drug transporters such as P-glycoprotein on the pharmacokinetics of tacrolimus to understand the precise absorption profile. In addition, the number of patients for each CYP3A5 genotype would be not enough to detect the difference by the CYP3A5 genotypes considering the large interindividual variability. A full PBPK model using the designed clinical data remains to be examined in a future study.

In conclusion, the effects of liver regeneration and hepatic and intestinal CYP3A5 genotypes on the pharmacokinetics of tacrolimus were quantitatively evaluated. Because liver function recovered immediately, dosing adjustment as a result of the liver regeneration might be needed only at 7 days after LDLT. The CL/F aspect could be classified into the following three patterns according to the CYP3A5 genotypes of the donor and recipient: (i) patients having L\*1/I\*1 showed high CL/F values, (ii) those having L\*1/I\*3 or L\*3/I\*1 indicated median CL/F values, and (iii) those having L\*3/I\*3 registered low CL/F values. As such, examining the CYP3A5 genotypes in the donor and recipient is useful for

designing the initial tacrolimus dosage in LDLT. However, because of the large interindividual and intraindividual variabilities of CL/F values in tacrolimus dosing, TDM is necessary to optimize the individual difference.

**Supporting Information.** Supplementary information accompanies this paper on the *CPT: Pharmacometrics & Systems Pharmacology* website ([www.psp-journal.com](http://www.psp-journal.com)).

**Figure S1.** Sensitive analysis about the fraction of drug unbound in the gut ( $f_{u,\text{gut}}$ ) vs. oral F in patients with each cytochrome P450 3A5 (CYP3A5) genotype.

**Figure S2.** Observed blood concentration of tacrolimus after LDLT patients in the model building data.

**Figure S3.** Effect of initial size of graft liver on the predicted blood concentration of tacrolimus immediately after LDLT.

**Table S1.** Characteristics of LDLT patients receiving tacrolimus therapy.

**Table S2.** Summary of the parameter values for tacrolimus simulation.

**Supplementary Information.** Equation used in Simcyp and NONMEM model code.

**Funding.** This study was supported in part by Grant-in Aid for the Scientific Research (KAKENHI) from the Japan Society for the Promotion of Science (JSPS) Grant numbers 16K08400 and 18H00394.

**Conflict of Interest.** The authors declared no competing interests for this work.

**Author Contributions.** K.I., I.Y., A.Y., and K.M. wrote the manuscript. K.I. and I.Y. designed the research. K.I., I.Y., T.T., M.U., A.Y., S.N., H.O., T.K., S.U., and K.M. performed the research. K.I. analyzed the data. K.I. contributed new reagents/analytical tools.

1. Venkataramanan, R. *et al.* Clinical pharmacokinetics of tacrolimus. *Clin. Pharmacokinet.* **29**, 404–430 (1995).
2. Staatz, C.E. & Tett, S.E. Clinical pharmacokinetics and pharmacodynamics of tacrolimus in solid organ transplantation. *Clin. Pharmacokinet.* **43**, 623–653 (2004).
3. Masuda, S. & Inui, K. An up-date review on individualized dosage adjustment of calcineurin inhibitors in organ transplant patients. *Pharmacol. Ther.* **112**, 184–198 (2006).
4. Kahan, B.D., Keown, P., Levy, G.A. & Johnston, A. Therapeutic drug monitoring of immunosuppressant drugs in clinical practice. *Clin. Ther.* **24**, 330–350 (2002).
5. Staatz, C.E., Goodman, L.K. & Tett, S.E. Effect of CYP3A and ABCB1 single nucleotide polymorphisms on the pharmacokinetics and pharmacodynamics of calcineurin inhibitors: part I. *Clin. Pharmacokinet.* **49**, 141–175 (2010).
6. Hebert, M.F. Contribution of hepatic and intestinal metabolism and P-glycoprotein to cyclosporine and tacrolimus oral drug delivery. *Adv. Drug Deliv. Rev.* **27**, 201–214 (1997).
7. Bekersky, I., Dressler, D., Alak, A., Boswell, G.W. & Mekki, Q.A. Comparative tacrolimus pharmacokinetics: novel versus mildly hepatically impaired subjects. *J. Clin. Pharmacol.* **41**, 628–635 (2001).
8. Haga, J. *et al.* Liver regeneration in donors and adult recipients after living donor liver transplantation. *Liver Transpl.* **14**, 1718–1724 (2008).
9. Yagi, S. *et al.* Impact of portal venous pressure on regeneration and graft damage after living-donor liver transplantation. *Liver Transpl.* **11**, 68–75 (2005).
10. Iida, T. *et al.* Assessment of liver graft function and regeneration by galactosyl-human serum albumin (99mTc-GSA) liver scintigraphy in adult living-donor liver transplantation. *Clin. Transplant.* **23**, 271–277 (2009).
11. Marcos, A. *et al.* Liver regeneration and function in donor and recipient after right lobe adult to adult living donor liver transplantation. *Transplantation* **69**, 1375–1379 (2000).
12. Akamatsu, N. *et al.* Regeneration and function of hemiliver graft: right versus left. *Surgery* **139**, 765–772 (2006).
13. Fukudo, M. *et al.* Population pharmacokinetic and pharmacogenomic analysis of tacrolimus in pediatric living-donor liver transplant recipients. *Clin. Pharmacol. Ther.* **80**, 331–345 (2006).
14. Antignac, M. *et al.* Population pharmacokinetics of tacrolimus in full liver transplant patients: modelling of the post-operative clearance. *Eur. J. Clin. Pharmacol.* **61**, 409–416 (2005).
15. Fukatsu, S. *et al.* Population pharmacokinetics of tacrolimus in adult recipients receiving living-donor liver transplantation. *Eur. J. Clin. Pharmacol.* **57**, 479–484 (2001).
16. Uesugi, M. *et al.* Impact of cytochrome P450 3A5 polymorphism in graft livers on the frequency of acute cellular rejection in living-donor liver transplantation. *Pharmacogenet. Genomics* **24**, 356–366 (2014).
17. Fukudo, M. *et al.* Impact of MDR1 and CYP3A5 on the oral clearance of tacrolimus and tacrolimus-related renal dysfunction in adult living-donor liver transplant patients. *Pharmacogenet. Genomics* **18**, 413–423 (2008).
18. Huang, S.M. & Rowland, M. The role of physiologically based pharmacokinetic modeling in regulatory review. *Clin. Pharmacol. Ther.* **91**, 542–549 (2012).
19. Bruggeman, F.J. & Westerhoff, H.V. The nature of systems biology. *Trends Microbiol.* **15**, 45–50 (2007).
20. Sager, J.E., Yu, J., Ragueneau-Majlessi, I. & Isoherranen, N. Physiologically based pharmacokinetic (PBPK) modeling and simulation approaches: a systematic review of published models, applications, and model verification. *Drug Metab. Dispos.* **43**, 1823–1837 (2015).
21. Hashi, S. *et al.* Assessment of four methodologies (microparticle enzyme immunoassay, chemiluminescent enzyme immunoassay, affinity column-mediated immunoassay, and flow injection assay-tandem mass spectrometry) for measuring tacrolimus blood concentration in Japanese liver transplant recipients. *Transplant. Proc.* **46**, 758–760 (2014).
22. Gertz, M., Houston, J.B. & Galetin, A. Physiologically based pharmacokinetic modeling of intestinal first-pass metabolism of CYP3A substrates with high intestinal extraction. *Drug Metab. Dispos.* **39**, 1633–1642 (2011).

23. Gertz, M., Harrison, A., Houston, J.B. & Galetin, A. Prediction of human intestinal first-pass metabolism of 25 CYP3A substrates from in vitro clearance and permeability data. *Drug Metab. Dispos.* **38**, 1147–1158 (2010).
24. Dai, Y. *et al.* Effect of CYP3A5 polymorphism on tacrolimus metabolic clearance in vitro. *Drug Metab. Dispos.* **34**, 836–847 (2006).
25. Barter, Z.E. *et al.* Determination of a quantitative relationship between hepatic CYP3A5\*1/\*3 and CYP3A4 expression for use in the prediction of metabolic clearance in virtual populations. *Biopharm. Drug Dispos.* **31**, 516–532 (2010).
26. Achour, B., Barber, J. & Rostami-Hodjegan, A. Expression of hepatic drug-metabolizing cytochrome p450 enzymes and their intercorrelations: a meta-analysis. *Drug Metab. Dispos.* **42**, 1349–1356 (2014).
27. Shiner, L.B. & Beal, S.L. Some suggestions for measuring predictive performance. *J. Pharmacokinet. Biopharm.* **9**, 503–512 (1981).
28. Tateishi, T. *et al.* No ethnic difference between Caucasian and Japanese hepatic samples in the expression frequency of CYP3A5 and CYP3A7 proteins. *Biochem. Pharmacol.* **57**, 935–939 (1999).
29. Lin, Y.S. *et al.* Co-regulation of CYP3A4 and CYP3A5 and contribution to hepatic and intestinal midazolam metabolism. *Mol. Pharmacol.* **62**, 162–172 (2002).
30. King, B.P., Leathart, J.B., Mutch, E., Williams, F.M. & Daly, A.K. CYP3A5 phenotype-genotype correlations in a British population. *Br. J. Clin. Pharmacol.* **55**, 625–629 (2003).
31. Press, R.R. *et al.* Explaining variability in tacrolimus pharmacokinetics to optimize early exposure in adult kidney transplant recipients. *Ther. Drug Monit.* **31**, 187–197 (2009).
32. Woillard, J. *et al.* Population pharmacokinetic model and Bayesian estimator for two tacrolimus formulations—twice daily Prograf and once daily Advagraf. *Br. J. Clin. Pharmacol.* **71**, 391–402 (2011).
33. Passey, C. *et al.* Dosing equation for tacrolimus using genetic variants and clinical factors. *Br. J. Clin. Pharmacol.* **72**, 948–957 (2011).
34. Han, N. *et al.* Prediction of the tacrolimus population pharmacokinetic parameters according to CYP3A5 genotype and clinical factors using NONMEM in adult kidney transplant recipients. *Eur. J. Clin. Pharmacol.* **69**, 53–63 (2013).
35. Zuo, X. *et al.* Effects of CYP3A4 and CYP3A5 polymorphisms on tacrolimus pharmacokinetics in Chinese adult renal transplant recipients: a population pharmacokinetic analysis. *Pharmacogenet. Genomics* **23**, 251–261 (2013).
36. Ogasawara, K., Chitnis, S.D., Gohh, R.Y., Christians, U. & Akhlaghi, F. Multidrug resistance-associated protein 2 (MRP2/ABCC2) haplotypes significantly affect the pharmacokinetics of tacrolimus in kidney transplant recipients. *Clin. Pharmacokinet.* **52**, 751–762 (2013).
37. Han, N. *et al.* Population pharmacokinetic-pharmacogenetic model of tacrolimus in the early period after kidney transplantation. *Basic Clin. Pharmacol. Toxicol.* **114**, 400–406 (2014).
38. Størset, E. *et al.* Importance of hematocrit for a tacrolimus target concentration strategy. *Eur. J. Clin. Pharmacol.* **70**, 65–77 (2014).
39. Bergmann, T., Hennig, S., Barraclough, K.A., Isbel, N.M. & Staatz, C.E. Population pharmacokinetics of tacrolimus in adult kidney transplant patients: impact of CYP3A5 genotype on starting dose. *Ther. Drug Monit.* **36**, 62–70 (2014).
40. Størset, E. *et al.* Improved prediction of tacrolimus concentrations early after kidney transplantation using theory-based pharmacokinetic modelling. *Br. J. Clin. Pharmacol.* **78**, 509–523 (2014).
41. Fukudo, M. *et al.* Forecasting of blood tacrolimus concentrations based on the Bayesian method in adult patients receiving living-donor liver transplantation. *Clin. Pharmacokinet.* **42**, 1161–1178 (2003).
42. Jacobson, P., Ng, J., Ratanatharathom, V., Uberti, J. & Brundage, R.C. Factors affecting the pharmacokinetics of tacrolimus (FK506) in hematopoietic cell transplant (HCT) patients. *Bone Marrow Transplant.* **28**, 753–758 (2001).
43. Antignac, M., Barrou, B., Farinotti, R., Lechat, P. & Urien, S. Population pharmacokinetics and bioavailability of tacrolimus in kidney transplant patients. *Br. J. Clin. Pharmacol.* **64**, 750–757 (2007).
44. Floren, L.C. *et al.* Tacrolimus oral bioavailability doubles with coadministration of ketoconazole. *Clin. Pharmacol. Ther.* **62**, 41–49 (1997).
45. Custodio, J.M., Wu, C.Y. & Benet, L.Z. Predicting drug absorption, absorption/elimination/transporter interplay and the role of food on drug absorption. *Adv. Drug Deliv. Rev.* **60**, 717–733 (2008).

© 2019 The Authors *CPT: Pharmacometrics & Systems Pharmacology* published by Wiley Periodicals, Inc. on behalf of the American Society for Clinical Pharmacology and Therapeutics. This is an open access article under the terms of the Creative Commons Attribution Non-Commercial License, which permits use, distribution and reproduction in any medium, provided the original work is properly cited and is not used for commercial purposes.